Astron. Astrophys. 355, 187–193 (2000)

ASTRONOMY AND ASTROPHYSICS

The infrared spectrum of the Be star γ Cassiopeiae*

S. Hony[1], L.B.F.M. Waters[1,2], P.A. Zaal[1], A. de Koter[1], J.M. Marlborough[3], C.E. Millar[3], N.R. Trams[4], P.W. Morris[1], and Th. de Graauw[5]

[1] Astronomical Institute Anton Pannekoek, University of Amsterdam, Kruislaan 403, 1098 SJ Amsterdam, The Netherlands
[2] Instituut voor Sterrenkunde, K.U. Leuven, Celestijnenlaan 200B, 3001 Heverlee, Belgium
[3] Department of Physics and Astronomy, University of Western Ontario, London, Ontario N6A 3K7, Canada
[4] Integral Science Operations, Astrophysics Division, Space Science Department of ESA, ESTEC, P.O. Box 299, 2200 AG Noordwijk, The Netherlands
[5] SRON Laboratory for Space Reserach, P.O. Box 800, 9700 AV Groningen, The Netherlands

Received 10 June 1999 / Accepted 8 October 1999

Abstract. We present the 2.4−45 μm ISO-SWS spectrum of the Be star γ Cas (B0.5 IVe). The spectrum is characterised by a thermal continuum which can be well fit by a power-law $S_\nu \propto \nu^{0.99}$ over the entire SWS wavelength range. For an isothermal disc of ionized gas with constant opening angle, this correponds to a density gradient $\rho(r) \propto r^{-2.8}$. We report the detection of the Humphreys (6-∞) bound-free jump in emission at 3.4 μm. The size of the jump is sensitive to the electron temperature of the gas in the disc, and we find T $\approx$ 9 000 K, i.e. much lower than the stellar effective temperature (25 000-30 000 K). The spectrum is dominated by numerous emission lines, mostly from H I, but also some He I lines are detected. Several spectral features cannot be identified. The line strengths of the H I emission lines do not follow case B recombination line theory. The line strengths and widths suggest that many lines are optically thick and come from an inner, high density region with radius 3-5 R_* and temperature above that of the bulk of the disc material. Only the α, β and γ transitions of the series lines contain a contribution from the outer regions. The level populations deviate significantly from LTE and are highly influenced by the optically thick, local (disc) continuum radiation field. The inner disc may be rotating more rapidly than the stellar photosphere.

Key words: stars: circumstellar matter – stars: emission-line, Be – stars: individual: γ Cas – stars: mass-loss – infrared: stars

1. Introduction

Be stars are rapidly rotating main sequence or giant stars that are characterized by the presence of (variable) Hα emission, caused by high-density circumstellar gas. Often the Hα line profile is double-peaked and its width correlates with the projected rotational velocity ($v \sin i$) of the underlying star (e.g. Dachs et al. 1986). At infrared and radio wavelengths, the continuum energy distribution of Be stars is dominated by free-free and bound-free emission from the high-density circumstellar gas, which also causes the Hα emission. Direct imaging of the circumstellar material at radio wavelengths (Dougherty & Taylor 1992) and in the Hα line, (e.g. Stee et al. 1998) shows that the gas is in a disc-like geometry. This flattened geometry is also evident from the optical continuum linear polarisation (e.g. Poeckert et al. 1979) due to electron scattering.

The physical mechanism responsible for the disc-like geometry is related to the rapid rotation of the star. Models proposed in the literature include the wind compressed disc model (Bjorkman & Cassinelli 1993), viscocity-driven outflow in the equatorial regions (Okazaki 1999) and non-radial pulsations (Vogt et al. 1983). Which of these models is correct can be tested by investigating the density and kinematical structure of the disc. We use the infrared spectral region to explore the structure of Be star discs. At these wavelengths disc emission dominates the spectrum, and a rich hydrogen and helium emission line spectrum is available. The infrared lines probe the inner regions of the disc, and their strength and width are important diagnostic tools for the density and kinematical structure of the disc. Ground-based infrared spectra of γ Cas were previously reported by e.g. Chalabaev & Maillard (1983), Lowe et al. (1985) and Hamann & Simon (1987). The Infrared Space Observatory (ISO) (Kessler et al. 1996) with its Short Wavelength Spectrometer (SWS) (De Graauw et al. 1996) is very well suited to explore the infrared part of the spectrum of Be stars.

In this study we present a preliminary analysis of the ISO-SWS spectrum of one of the brightest and best studied Be stars in the sky, γ Cas (B0.5IVe). We will show that the H I emission line spectrum of γ Cas is not well represented by Menzel case B recombination line theory. Many line fluxes correlate with the local continuum and are independent of the intrinsic line strength (Einstein A coefficient). The observed line fluxes and widths suggest that these lines are formed in an inner region with well-determined size, and that only the intrinsically strongest lines have a contribution from outer layers. This paper

Send offprint requests to: S. Hony (hony@astro.uva.nl)

* based on observations obtained with ISO, an ESA project with instruments funded by ESA Member states (especially the PI countries: France, Germany, the Netherlands and the United Kingdom) with the participation of ISAS and NASA

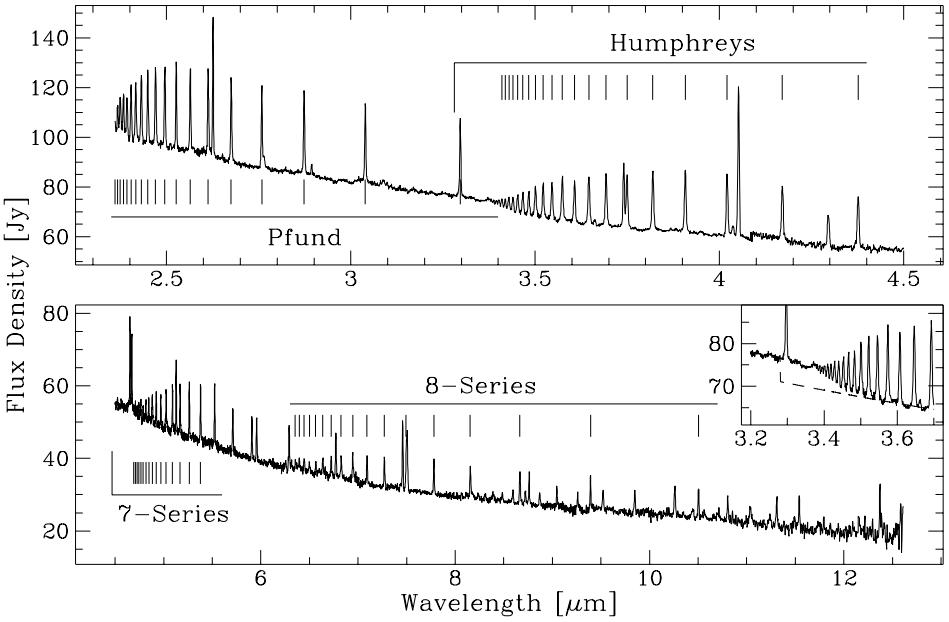

Fig. 1. SWS AOT01 speed 4 spectrum of γ Cas between 2 and 12 μm. The spectrum is dominated by numerous emission lines from hydrogen. A few He lines are also observed. The inset shows the region aroud the Humphreys jump. The dashed line shows the jump in the continuum level due to the jump in bound−free opacity near 3.4 μm.

is organized as follows. In Sect. 2 we briefly discuss the observations and data reduction. Sect. 3 discusses the continuum and Sect. 4 deals with the line spectrum. Sect. 5 discusses some implications of our measurements for the structure of the disc of γ Cas.

2. Observations and data analysis

The Be star γ Cas was observed with the SWS on board ISO on July 22nd, 1996, as part of the SWS guaranteed time programme BESTARS. A full spectral scan (2.4-45 μm) using Astronomical Observation Template (AOT) no. 1, speed 4 (De Graauw et al. 1996) was obtained, while also several AOT02 line scans were taken. The observations were reduced using the SWS Interactive Analysis (IA^3) software package, with calibration files equivalent to pipeline version 7.0. Further processing consisted of bad data removal and rebinning on an equidistant wavelength grid. The flux levels are accurate to within 5 per cent for the wavelengths shortward of 7 μm. The observations between 7 and 12 μm (band 2C) suffer from memory effects; this has little influence on the measured line properties but does increase the uncertainty of the continuum flux level to 15 per cent. At even longer wavelengths the signal to noise ratio decreases dramatically and only the strongest lines can be measured with reasonable accuracy. Most of the emission lines are partially resolved with a ratio of FWHM to the FWHM of the instrumental profile between 1.4-3.5. Only 6 of the emission lines are considered unresolved having this ratio below 1.4. Since the SWS instrumental profile is approximately Gaussian (Valentijn et al. 1996) and the observed lines are well fitted by Gaussians, we estimate the original line width from:

$$w_{\rm obs}{}^2 = w_{\rm org}{}^2 + w_{\rm inst}{}^2, \quad (1)$$

where $w_{\rm obs}$ is the observed FWHM, $w_{\rm org}$ is the original FWHM and $w_{\rm inst}$ is the FWHM of the instrumental profile. The latter value varies with wavelength. To determine $w_{\rm inst}$, we use measured line widths of emission lines of planetary nebulae; NGC 7027 and NGC 6302, observed in the same observing mode. No significant line profile variations are observed. We show the final AOT01 spectrum in Fig. 1.

3. The continuum energy distribution

The continuum energy distribution of γ Cas at IR wavelengths is dominated by free-free and bound-free emission from the ionized part of the circumstellar gas (e.g. Poeckert & Marlborough 1978; Waters et al. 1987). The stellar contribution to the total flux is about 20 per cent at 2.4 μm, based on extrapolation of a Kurucz model atmosphere fitted to the UV continuum (Telting et al. 1993). The spectrum can be well represented by a single power-law, $S_\nu \propto \nu^\alpha$, with $\alpha = 0.99 \pm 0.05$. This spectral slope is slightly, but significantly flatter, than that derived by Waters et al. (1987), based on IRAS broad-band photometry taken in 1983. We have used the simple isothermal disc model of Waters (1986) to estimate the radial density gradient in the disc, assuming a power-law $\rho(r) = \rho_0(r/R_*)^{-n}$, and find $n = 2.8 \pm 0.1$. The value of ρ_0 depends on the assumed opening angle θ of the disc, as well as on the stellar radius and disc temperature. We use $R_* = 10\ R_\odot$ and $T_{\rm disc} = 10^4$ K (see below). Analysis of the optical linear polarisation and interferometric imaging of ζ Tau (Wood et al. 1997) suggests a half opening angle of 2.5°. We use a 1° half opening angle. The derived density at the stellar surface is $\rho_0 = 3.5\times10^{-11}$ g cm^{-3}; an emission measure EM = 1.5×10^{61} cm^{-3} was found.

There are some wavelength ranges that show a deviation from the power-law behavior of the continuum discussed above. Near 3.28 μm the merging of the emission lines of the Humphreys series, with lower quantum level $n = 6$, causes a jump. This Humphreys jump (seen in emission), which is similar to the Balmer jump at optical wavelengths, can be used to

derive the average electron temperature of the emitting region. The difference in flux on both sides of the Humphreys jump is caused by a discontinuity in bound-free ($\kappa_{\rm ff+bf}$) opacity of the gas in the disc. We write for the total continuum opacity.

$$\kappa_{\rm ff+bf} \propto \lambda^2 \times (1 - e^{-ch/\lambda kT})/(ch/\lambda kT) \times T^{-3/2} \times \{g(\lambda, T) + b(\lambda, T)\}, \quad (2)$$

where g(λ,T) and b(λ,T) are the free-free and bound-free gaunt factors, respectively. b(λ,T) is a sensitive function of the temperature: the jump in b(λ,T) (and in flux) increases towards lower electron temperature. The change in g(λ,T) is negligible over the wavelength range of interest. The jump in b(λ,T) is thus a diagnostic of the temperature in the disc. We use the following method to determine the size of this jump: We define the normalized excess flux as $Z_\lambda - 1 = (F_\lambda - F_{\lambda,*})/F_{\lambda,*}$, where $F_{\lambda,*}$ is the stellar photospheric flux, see Fig. 2. $Z_\lambda - 1$ is normalized to the source function of the gas in the disc modulo a constant since both the disc and the star radiate in the Rayleigh-Jeans limit in this wavelength regime and thus have the same wavelength dependence. On the blue side of the discontinuity b(λ,T) has a certain value, with a corresponding value of $\kappa_{\rm ff+bf}$, of $\tau_{\rm ff+bf}$ for each line of sight through the disc and thus a corresponding value of $Z_\lambda - 1$. Beyond the discontinuity there is a drop in b(λ,T), $\kappa_{\rm ff+bf}$, $\tau_{\rm ff+bf}$ and $Z_\lambda - 1$. Since there is a wide range of $\tau_{\rm ff+bf}$ for different lines of sight $Z_\lambda - 1$ is *not* a simple function of b(λ,T). However $\kappa_{\rm ff+bf}$ steadily increases with wavelength, e.g. Eq. 2, and thus there is a wavelength (λ') where the loss in b(λ,T) is compensated by the increase in λ. At λ' the $\kappa_{\rm ff+bf}$ is equal to the previous value, so $\tau_{\rm ff+bf}$ and $Z_\lambda - 1$ are also equal. We can determine λ' directly from the observations, e.g. Fig. 2.

Using $\lambda' = 3.470 \pm 0.005$ μm and the gaunt factors calculated by Waters & Lamers (1984) we find an electron temperature in the disc of 9 500 $\pm$ 1 000 K. This temperature would cause a weak but measurable jump at the Hansen-Strong series limit (near 4.5 μm) but none is observed. However, we note that near this wavelength two strong H I lines are present that may mask an otherwise detectable jump. The disc temperature agrees well with a density-weighted temperature of 10 700 K derived by Millar & Marlborough (1998) from an energy balance calculation using the Poeckert & Marlborough model for the disc of γ Cas. Note that the inner regions of the disc may have considerably higher temperatures, because this method is insensitive to contributions of those parts of the highest density parts of the disc where the continuum is optically thick. (see also Sect. 4). A second region which deviates from the power-law is near 4.3 μm. We cannot find a reasonable identification for this spectral feature. The CO_2 stretch mode band is at 4.27 μm. However, the interstellar extinction towards γ Cas is very low which implies that we must rule out this possibility.

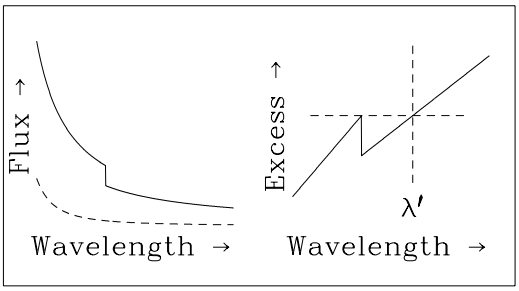

Fig. 2. Schematic representation of the method used to derive the temperature from the Humphreys jump. On the left the observed flux (drawn line) and the photospheric contribution (dotted line) are shown. on the right the normalized excess flux is shown. Also indicated is the wavelength(λ') longward of the jump where the excess is equal to the excces at the jump.

4. The emission lines

The entire SWS spectral region, but especially bands 1 and 2 (2.4-12 μm), is dominated by strong and partially resolved emission lines. The vast majority of these lines are H I recombination lines. We find the series limit of the Humphreys and Hansen-Strong series, as well as those from lower levels 8, 9 and 10. Several lines with lower levels above 10 were also identified. We find a few He I lines (notably at 2.4861, 2.5729, 4.2960 and 4.0367 μm). No forbidden lines could be found, although several emission features are unidentified and could perhaps be attributed to forbidden lines. The strongest unidentified line is at 2.8934 μm, close to the 2.8964 [Ni II] line. The lack of fine-structure lines is consistent with the optical spectrum of γ Cas. It is likely that the high density of the ionized gas causes collisional de-excitation of the fine-structure transitions. This situation is markedly different for the hypergiant P Cygni, whose infrared spectrum is also dominated by H I recombination lines from circumstellar gas, but which also shows prominent emission from e.g. [Fe II], [Ni II] and [Si II] in its ISO-SWS spectrum (Lamers et al. 1996).

We have measured the line fluxes with respect to both the *local* continuum and the *stellar* photospheric continuum at line centre. The measured line properties are given in Table 1. In Fig. 4 we show the resulting curve of growth for the emission lines, where we plot the equivalent width EW divided by wavelength versus log $X_{\rm line}$. This last quantity is proportional to the line optical depth (Zaal et al. 1995). The observed line fluxes (Fig. 3) are all much smaller (a factor 10 or more) than expected on the basis of the continuum emission measure determination and the optically thin case B recombination line predictions (Hummer & Storey 1987). This shows that even for the weakest lines the emission is optically thick: the combined line and continuum opacity is much larger than 1. This is not surprising given the shape of the continuum energy distribution; Waters et al. (1991) show that the continuum becomes optically thick near 0.8 μm.

The shape of the empirical curve of growth is very different from that expected on the basis of LTE line formation in a rotating, partially optically thick disc. Model calculations show that under these conditions the curve of growth has a linear part (where line emission is optically thin and proportional to line strength), and a power-law part whose slope depends on the radial density gradient of the

Table 1. Properties of hydrogenic emission lines. λ is the peak wavelength of the Gaussian fit. Typical errors on these are 1/2500th of the wavelength. $width$ is the FWHM of the line after deconvolution. I is the integrated line-flux. $cont.$ is the mean continuum level underneath the line. The errors on the continuum level are dominated by the absolute flux calibration uncertainty of the SWS instrument.

(1) $trans.$ –	(2) λ $[\mu m]$	(3) $width$ $[kms^{-1}]$	(4) I $[W/m^2]$	(5) $cont.$ $[Jy]$	(6) $trans.$ –	(7) λ $[\mu m]$	(8) $width$ $[kms^{-1}]$	(9) I $[W/m^2]$	(10) $cont.$ $[Jy]$
5–4	4.052	254 ± 42	5.45e-14 ± 6%	61± 6%	10–7	8.761	249 ± 39	3.70e-15 ±10%	24±10%
6–4	2.626	226 ± 56	7.14e-14 ± 5	91± 5	12–7	6.772	364 ± 40	8.21e-15 ± 8	35± 8
6–5	7.460	220 ± 65	9.51e-15 ± 8	28± 8	13–7	6.292	414 ± 41	1.02e-14 ± 7	37± 7
7–5	4.654	200 ± 43	1.58e-14 ± 6	56± 6	14–7	5.957	303 ± 64	9.11e-15 ± 7	40± 7
8–5	3.741	267 ± 48	2.69e-14 ± 6	64± 5	15–7	5.712	376 ± 56	1.12e-14 ± 7	42± 7
9–5	3.297	284 ± 23	3.33e-14 ± 5	77± 5	16–7	5.525	393 ± 13	1.34e-14 ± 7	45± 6
10–5	3.039	273 ± 32	3.73e-14 ± 5	80± 5	17–7	5.380	367 ± 16	1.21e-14 ± 7	46± 6
11–5	2.873	309 ± 33	4.53e-14 ± 5	84± 5	18–7	5.264	335 ± 18	1.13e-14 ± 7	47± 6
12–5	2.758	313 ± 36	4.73e-14 ± 5	86± 5	19–7	5.169	390 ± 16	1.09e-14 ± 7	48± 6
13–5	2.675	324 ± 37	5.37e-14 ± 5	88± 5	20–7	5.091	396 ± 17	1.16e-14 ± 6	49± 6
14–5	2.613	347 ± 12	5.20e-14 ± 5	95± 5	21–7	5.026	457 ± 15	1.11e-14 ± 6	49± 6
15–5	2.564	340 ± 13	5.38e-14 ± 5	95± 5	22–7	4.971	441 ± 16	9.04e-15 ± 7	50± 6
16–5	2.526	344 ± 14	5.68e-14 ± 5	96± 5	23–7	4.923	425 ± 17	8.34e-15 ± 7	50± 6
17–5	2.495	379 ± 13	5.53e-14 ± 5	97± 5	24–7	4.883	551 ± 13	8.86e-15 ± 7	51± 6
18–5	2.470	407 ± 12	5.66e-14 ± 5	98± 5	25–7	4.847	441 ± 17	6.69e-15 ± 7	51± 6
19–5	2.449	386 ± 13	5.17e-14 ± 5	98± 5	26–7	4.817	420 ± 18	5.18e-15 ± 8	52± 6
20–5	2.431	390 ± 13	4.83e-14 ± 5	99± 5	27–7	4.789	455 ± 17	4.39e-15 ± 8	52± 6
21–5	2.416	447 ± 12	4.79e-14 ± 5	99± 5	28–7	4.765	551 ± 14	5.45e-15 ± 8	52± 6
22–5	2.404	417 ± 13	4.24e-14 ± 5	100± 5	29–7	4.744	706 ± 11	5.59e-15 ± 8	52± 6
23–5	2.393	414 ± 13	3.20e-14 ± 5	100± 5	12–8	10.504	282 ± 22	2.88e-15 ±13	20±12
24–5	2.383	491 ± 11	4.03e-14 ± 5	101± 5	13–8	9.393	204 ± 41	2.97e-15 ±11	23±11
7–6	12.371	313 ± 13	4.34e-15 ±15	15±15	14–8	8.666	339 ± 29	4.40e-15 ±10	24±10
9–6	5.908	295 ± 67	8.81e-15 ± 7	41± 7	15–8	8.156	345 ± 33	4.69e-15 ±10	26± 9
10–6	5.129	325 ± 20	1.46e-14 ± 6	48± 6	16–8	7.781	291 ± 44	4.87e-15 ± 9	27± 9
11–6	4.673	304 ± 27	1.57e-14 ± 6	56± 6	18–8	7.272	252 ± 60	4.24e-15 ± 9	29± 8
12–6	4.377	326 ± 30	1.98e-14 ± 6	57± 6	19–8	7.093	321 ± 49	4.83e-15 ± 9	30± 8
13–6	4.171	348 ± 32	2.33e-14 ± 6	61± 6	20–8	6.947	484 ± 28	5.67e-15 ± 8	34± 8
14–6	4.021	304 ± 35	2.52e-14 ± 6	60± 6	21–8	6.827	445 ± 32	4.48e-15 ± 9	35± 8
15–6	3.908	332 ± 35	2.73e-14 ± 6	62± 5	22–8	6.724	376 ± 39	3.67e-15 ± 9	36± 8
16–6	3.820	350 ± 35	2.77e-14 ± 6	63± 5	23–8	6.639	421 ± 36	3.47e-15 ± 9	36± 7
17–6	3.750	360 ± 35	2.68e-14 ± 6	64± 5	24–8	6.566	528 ± 29	3.82e-15 ± 9	35± 7
18–6	3.693	372 ± 35	2.63e-14 ± 6	65± 5	26–8	6.447	671 ± 24	4.53e-15 ± 8	36± 7
19–6	3.646	392 ± 34	2.54e-14 ± 6	65± 5	15–9	11.539	275 ± 18	2.71e-15 ±14	17±14
20–6	3.607	344 ± 40	2.08e-14 ± 6	66± 5	16–9	10.805	301 ± 19	2.26e-15 ±14	20±13
21–6	3.574	387 ± 36	2.06e-14 ± 6	67± 5	17–9	10.261	431 ± 15	4.07e-15 ±12	21±12
22–6	3.546	380 ± 38	1.95e-14 ± 6	67± 5	18–9	9.848	292 ± 25	2.36e-15 ±12	22±11
23–6	3.522	408 ± 36	1.69e-14 ± 6	67± 5	19–9	9.522	337 ± 24	2.21e-15 ±12	23±11
24–6	3.501	466 ± 32	1.75e-14 ± 6	68± 5	20–9	9.261	364 ± 23	2.18e-15 ±12	22±10
25–6	3.483	476 ± 31	1.49e-14 ± 6	68± 5	21–9	9.047	283 ± 32	2.05e-15 ±12	23±10
26–6	3.467	438 ± 34	1.18e-14 ± 6	68± 5	22–9	8.870	422 ± 22	1.96e-15 ±12	24±10
27–6	3.452	621 ± 24	1.40e-14 ± 6	69± 5	23–9	8.721	416 ± 24	1.88e-15 ±12	24±10
28–6	3.440	639 ± 24	1.29e-14 ± 6	69± 5	24–9	8.594	375 ± 27	1.82e-15 ±12	25±10
29–6	3.429	641 ± 24	1.08e-14 ± 6	69± 5	25–9	8.485	430 ± 24	1.36e-15 ±14	25± 9
9–7	11.309	394 ± 13	2.96e-15 ±14	17±13	20–10	12.156	439 ± 9	1.91e-15 ±16	16±15

gas (Zaal et al. 1995), see also Wellmann (1952). The observed curve of growth however shows a very steep rise of EW/λ with X_{line} up to log $X_{line} \approx -36.5$, followed by a flat part for $-36.5 <$ log $X_{line} < -35.0$ whose slope is close to zero, i.e. much smaller than 0.4 expected on the basis of the density gradient derived from the continuum free-free and bound-free excess. Finally, a rising part for the strongest lines in the spectrum (log $X_{line} > -35.0$) is seen. The flat part of the curve of growth is surprising and suggests that these lines have saturated and are formed in a region with a well-defined outer radius. We note that the size of this region is not the same for every series, but increases with lower quantum level.

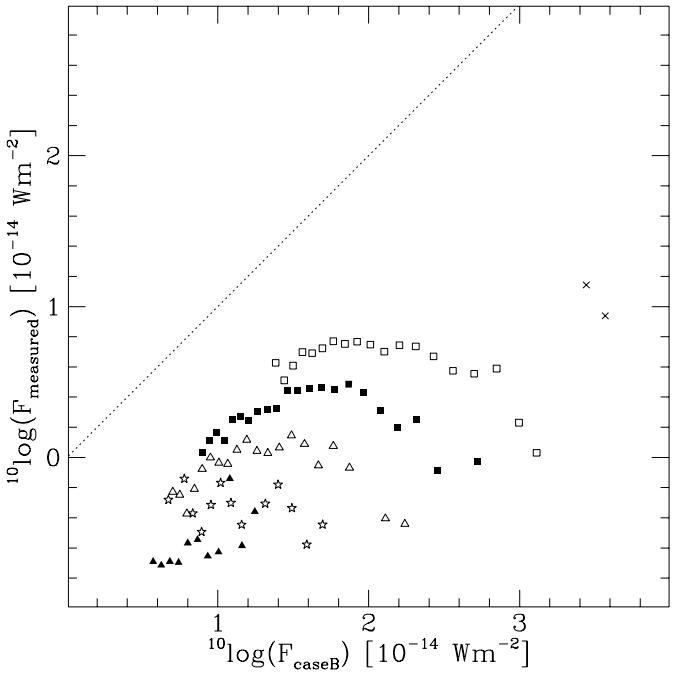

Fig. 3. Comparison of measured line strengths with predictions based on optically thin case B recombination theory. The dotted line denotes the locus where the measured fluxes would equal the predictions. The crosses correspond to Brackett α and β, the open squares to the Pfund series, the filled squares to the Humphreys series, the open triangles to the Hansen-Strong series, the stars to $n = 8$, and the filled triangles to $n = 9$.

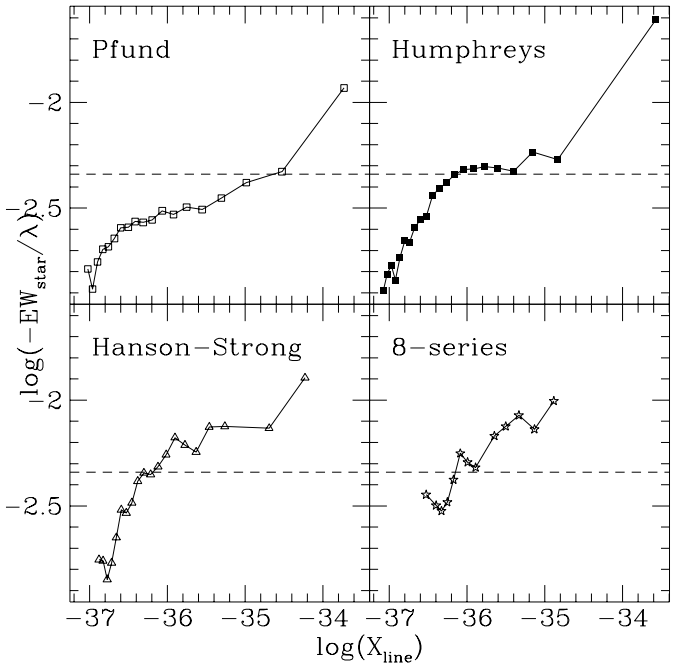

Fig. 4. Measured line fluxes, expressed in equivalent width (EW/λ) with respect to the stellar continuum versus line opacity. The line fluxes are independent of line strength between log $X_{\rm line} \approx -36$ and -35.

In order to understand better the nature of the line formation in γ Cas, we show in Fig. 5 the line strength $\overline{EW}/\lambda$, where $\overline{EW}$ is the line equivalent width measured with respect to the *local* continuum, as a function of wavelength. Also shown in Fig. 5 is the line FWHM versus wavelength. Both $\overline{EW}/\lambda$ and the FWHM show a characteristic wavelength dependence: for each series, $\overline{EW}/\lambda$ increases and then saturates to a value of 5-6$\times10^{-4}$, while the line FWHM decreases and reaches a roughly constant value of 250-300 km s^{-1}. In other words, the lines reach a constant line over continuum ratio of about 1.3 at a constant FWHM of 250-300 km s^{-1}. Only the α and β lines of each series deviate from this behaviour: their line over continuum ratio is larger and their FWHM smaller.

The decrease of FWHM with increasing line strength is expected for lines formed in a rotating disc in which the rotational velocity decreases with distance; as more line flux is coming from the outer, more slowly rotating regions, the line width will decrease. This is direct proof of the rotating nature of the line emitting region. It is remarkable that the weakest lines of each series have a very high FWHM of more than 550 km s^{-1}. Such high velocities are not expected given the photospheric v sin i of 230 km s^{-1} (Slettebak 1982). This suggests that the inner disc is rotating more rapidly than the star. However, line broadening due to electron scattering could also cause these large line widths, but we do not observe prominent electron scattering wings.

If we assume that the line and continuum source functions are equal, no line emission from the layers with $\tau_{\rm ff} > 1$ should be detectable. However, the large line width of the weakest lines strongly suggests that this line emission is originating from rapidly rotating parts of the disc. The fact that the line FWHM decreases with increasing line strength shows that the broad, weak lines are formed closest to the star. In the 2.5 to 7 μm wavelength region, where most of the weakest lines in Fig. 5 are located, the continuum is optically thick out to a radius of 2.5 to 3 R$_*$. Assuming Keplerian rotation in the disc, the part of the disc which is not optically thick for continuum radiation rotates at projected speeds less than about $v_0 \sin i/1.7$, where v_0 is the Keplerian velocity of the disc at the stellar surface. Using reasonable values for the mass and radius for a B0.5 IV star of R$_*$=10 R$_\odot$ and M$_*$=15 M$_\odot$, we find a maximum speed of about 220 km s^{-1}. Emission lines in the disc whose source function is equal to that of the continuum therefore should have *FWZI* less than 440 km s^{-1}, but even the FWHM of the weak lines is significantly higher than this. It is unlikely that rotational velocities are as high as 250-300 km s^{-1} as far out as 2.5-3 R$_*$, unless the rotational velocity field deviates significantly from Keplerian. We conclude that we detect line emission from those parts of the disc that are optically thick for continuum radiation, and hence the line source function in these inner regions must exceed that of the continuum (which is the Planck function at the local electron temperature). Several effects can cause such a larger source function: NLTE level populations, or an enhanced electron temperature near the upper part of the disc. If the latter effect is important, temperatures in the line forming regions

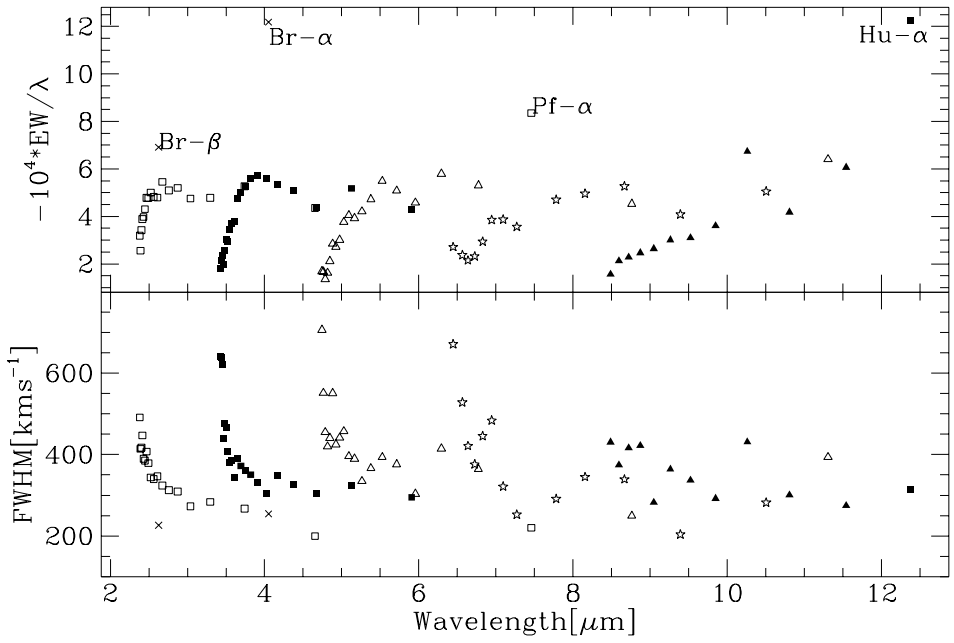

Fig. 5. *Top panel*: EW/λ of the H I lines in the ISO-SWS spectrum of γ Cas as a function of wavelength. Symbols are the same as in Fig. 3. The EWs have been determined with respect to the local continuum. The EWs for all series behave in a similar way. For moderately strong lines the EW/λ does not depend on wavelength and is about -5×10^{-4} irrespective of the series. Only the strongest lines of each series deviate from this trend. *Bottom panel*: observed full width at half maximum of the H I lines versus wavelength. The symbols refer to the same series as in the upper panel. The lines become narrower with increasing line strength as expected in a rapidly rotating disc in which the rotational velocity decreases with distance. The FWHM does not decrease further for moderately strong lines. These lines also show a constant EW/λ (upper panel).

may be as much as 30 per cent higher than in the bulk of the disc, since the stronger lines are 1.3 times the continuum.

As pointed out above, the observed line fluxes of every series first increase with intrinsic line strength, but then reach a constant value with respect to the local continuum, both in $\overline{EW}/\lambda$ and in the line to continuum ratio. This effect occurs for transitions from upper levels roughly between 15 and about 10, to lower levels between 9 and 5. The line fluxes are no longer determined by the intrinsic line strength, but by *the local continuum!* The contribution from outer regions, with lower rotational velocities, is absent. This can be seen from the FWHM's of the lines with constant line over continuum ratio, that no longer decrease but are constant at about 250-300 km s^{-1}. This could be due to a finite outer radius of the disc. However, the ISO-SWS spectrum as well as ISO-PHOT photometry at 90 μm (Trams et al., in preparation) show that there is no change in continuum slope over a wide wavelength range. Such a change in slope would be expected in the case of a finite outer radius. We conclude that the lack of line emission from the outer regions cannot be due to a finite outer disc radius. We note that the fact that the line to continuum ratio is constant for certain lines, irrespective of the strength of the local continuum and thus of the size of the continuum emitting region, also argues against a finite outer radius.

The lack of line flux from the outer regions therefore must be due to a change (decrease) in the line source function compared to the inner regions. For a certain range of intermediate energy levels in the atom, the optically thick IR free-free disc radiation field in the inner regions is able to maintain significant level populations, but these levels rapidly become de-populated when the local free-free continuum becomes optically thin. Therefore the line flux does not increase with intrinsic line strength (as do the weaker lines from high upper levels), but reaches a line over continuum ratio determined by the ratio of source functions of line and continuum.

5. Discussion

Hamann & Simon (1987) discuss the near-IR spectrum of γ Cas and note that the line flux ratios of the weak Pfund lines to the Brγ line are very difficult to reconcile with those of Brγ and Brα for any reasonable choice of radial density gradient in the disc. We confirm this result and show that it is a general property of the line fluxes of γ Cas to behave in a highly non-standard way, probably caused by a combination of non-LTE and temperature effects. We do not confirm the lack of correlation between line strength and line width noted by Hamann & Simon (1987); the ISO data clearly show such a correlation for all series in our spectrum. This may be due to the Earth atmosphere affecting the estimate of the weak high level Pfund series lines in the spectrum of Hamann & Simon. The line widths of their stronger lines (e.g. Brα) agree well with those of our spectrum. They also agree well with the line widths derived from high-resolution spectra published by Lowe et al. (1985) and Chalabaev & Maillard (1983).

The FWHM of the weakest H I lines (more than 500 km s^{-1}) significantly exceeds that of the photospheric $v \sin i$ of 230 km s^{-1}. While electron scattering may affect the width of the strongest lines (especially at short wavelengths where free-free opacities are small compared to the electron scattering opacity) the IR lines do not show evidence for prominent electron scattering wings. This suggests that the line width is mainly due to kinematical broadening, which would imply that the disc is rotating more rapidly than the underlying star (ignoring errors

in v $\sin$ i). This can only occur if some mechanism adds angular momentum to the material injected into the disc. We note that Hanuschik (1987) found line widths of weak Fe II emission lines in the optical spectra of Be stars that also significantly exceeded the width expected on the basis of the observed v $\sin$ i. Transfer of angular momentum may lead to spin-down of the star (Porter 1998). Using the formalism given by Porter (1998), and assuming a full opening angle of 2 degrees and ρ_0 of 3×10^{-11} g cm^{-3}, the outflow velocity in the disc near the star can be of the order of 1 km s^{-1} without significant spin-down of the star during its main sequence life time. Such a value is in agreement with the observed line shape.

The picture which emerges from our analysis of the infrared spectrum of γ Cas is that of a circumstellar region of very high density, perhaps exceeding 3 10^{-11} g cm^{-3}, which is rotating rapidly and whose rotational velocity decreases with distance. The rotational velocity in the disc near the star exceeds that of the photosphere. This region is heated by radiation from the central star, and the surface layers which directly absorb the stellar radiation field have higher temperatures than regions closer to the equatorial plane of the disc. While the weak lines originate from these dense, warm regions, only the strongest, α and β, lines of each series probe the outer portions of the disc.

Acknowledgements. LBFMW and AdK acknowledge financial support from an NWO *Pionier* grant. JMM acknowledges support from an NSERC grant. JMM and LBFMW acknowledge financial support from a NATO Collaborative Resarch Grant (CRG.941220). This work was supported by NWO Spinoza grant 08-0 to E.P.J. van den Heuvel. CEM acknowledges financial support from an NSERC postgraduate scholarship.

References

Bjorkman J.E., Cassinelli J.P., 1993, ApJ 409, 429
Chalabaev A., Maillard J.P., 1983, A&A 127, 279
Dachs J., Hanuschik R., Kaiser D., Rohe D., 1986, A&A 159, 276
De Graauw T., Haser L.N., Beintema D.A., et al., 1996, A&A 315, L49
Dougherty S.M., Taylor A.R., 1992, Nat 359, 808
Hamann F., Simon M., 1987, ApJ 318, 356
Hanuschik R.W., 1987, A&A 173, 299
Hummer D.G., Storey P.J., 1987, MNRAS 224, 801
Kessler M.F., Steinz J.A., Anderegg M.E., et al., 1996, A&A 315, L27
Lamers H.J.G.L.M., Najarro F., Kudritzki R.P., et al., 1996, A&A 315, L229
Lowe R.P., Moorhead J.M., Wehlau W.H., Barker P.K., Marlborough J.M., 1985, ApJ 290, 325
Millar C.E., Marlborough J.M., 1998, ApJ 494, 715+
Okazaki A.T., 1999, In: *IAU Colloq. 169*, in press
Poeckert R., Bastien P., Landstreet J.D., 1979, AJ 84, 812
Poeckert R., Marlborough J.M., 1978, ApJ 220, 940
Porter J.M., 1998, A&A 333, L83
Slettebak A., 1982, ApJS 50, 55
Stee P., Vakili F., Bonneau D., Mourard D., 1998, A&A 332, 268
Telting J.H., Waters L.B.F.M., Persi P., Dunlop S.R., 1993, A&A 270, 355
Valentijn E.A., Feuchtgruber H., Kester D.J.M., et al., 1996, A&A 315, L60
Vogt S.S., Penrod G.D., Soderblom D.R., 1983, ApJ 269, 250
Waters L.B.F.M., 1986, A&A 162, 121
Waters L.B.F.M., Cote J., Lamers H.J.G.L.M., 1987, A&A 185, 206
Waters L.B.F.M., Lamers H.J.G.L.M., 1984, A&AS 57, 327
Waters L.B.F.M., Marlborough J.M., Van Der Veen W.E.C., Taylor A.R., Dougherty S.M., 1991, A&A 244, 120
Wellmann P., 1952, *Zeitschrift Astrophys.* 30, 96
Wood K., Bjorkman K.S., Bjorkman J.E., 1997, ApJ 477, 926
Zaal P.A., Waters L.B.F.M., Marlborough J.M., 1995, A&A 299, 574